Thermophysical Analysis of Smectic A Domains Confined into a Thermoplastic Polymer Matrix

L. Bedjaoui-Alachaher [a] , F. Semdani [a] , R. Meziane [b] & U. Maschke [b]

[a] Laboratoire de Recherche sur les Macromolécules, Faculté des Sciences, University of Tlemcen, Tlemcen, Algeria

[b] Unité Matériaux et Transformations (UMET), UMR CNRS 8207, Université de Lille 1 – Sciences et Technologies, Villeneuve d'Ascq, France

PLEASE SCROLL DOWN FOR ARTICLE

Taylor & Francis
Taylor & Francis Group

Thermophysical Analysis of Smectic A Domains Confined into a Thermoplastic Polymer Matrix

L. BEDJAOUI-ALACHAHER,[1] F. SEMDANI,[1]
R. MEZIANE,[2] AND U. MASCHKE[2]

[1]Laboratoire de Recherche sur les Macromolécules, Faculté des Sciences, University of Tlemcen, Tlemcen, Algeria
[2]Unité Matériaux et Transformations (UMET), UMR CNRS 8207, Université de Lille 1 – Sciences et Technologies, Villeneuve d'Ascq, France

Cloud point measurements and calorimetric properties were considered for binary systems of polystyrene/4cyano-4'-n-octylbiphenyl (8CB), and deuterated polystyrene/8CB. The experimental phase diagrams were established using polarizing optical microscopy and differential scanning calorimetry. The experiments were realized in the range of temperatures from 25 to 75°C, in which the 8CB presents a smectic A structure, a nematic and an isotropic phase. The phase behavior of both systems were analyzed using a combination of the Flory-Huggins lattice model for isotropic mixing and the Maier-Saupe-McMillan theories for anisotropic ordering. A good agreement was obtained between theoretical considerations and experimental data.

Keywords Flory-Huggins; Maier-Saupe-McMillan; phase diagrams; polystyrene; smectic liquid crystal

1. Introduction

Polymer dispersed liquid crystals (PDLCs) are heterogeneous composite materials consisting of films with a Swiss-cheese morphology in which the liquid crystal (LC) molecules are confined into domains [1,2]. The phase separation process and the phase behavior are the main aspects governing the morphology of PDLC materials. Indeed, size, shape, spatial distribution and number density of LC domains, influence the electro-optical properties of the films. PDLCs represent an important new class of materials with potential applications in the areas of light shutters, flat panel displays, privacy windows, micro-lenses etc. [3,4]. In order to fabricate them it is important to understand their thermophysical properties [5]. In this context, we report some results concerning the study of binary blends of 8CB, which is a low molecular weight smectic A LC, and two well defined polymers: polystyrene

---

Address correspondence to U. Maschke, Unité Matériaux et Transformations (UMET), UMR CNRS 8207, Université de Lille 1 – Sciences et Technologies, 59655 Villeneuve d'Ascq Cedex, France. Tel.: 0033 3 20 33 63 81; Fax: 0033-3-20 43 43 45; E-mail: ulrich.maschke@univ-lille1.fr

(PS, $M_w = 44000$ g/mol) and deuterated polystyrene (dPS, $M_w = 59000$ g/mol). The blends were characterized using differential scanning calorimetry (DSC) and polarizing optical microscopy (POM) to investigate the thermophysical properties and the morphology of the composite materials.

The experimental data were analyzed in detail using a theoretical model that combines the Flory-Huggins theory [6] for isotropic mixing and the Maier-Saupe-McMillan theories for anisotropic ordering [7–9].

2. Experimental

2.1. *Materials*

PS 44000 was purchased from Aldrich (Saint Quentin Fallavier, France) and was used without purification. The second polymer was a completely deuterated polystyrene dPS 59000 which was prepared by Th. Wagner of the Max-Planck Institute of Polymer Research at Mainz/Germany. The weight average molecular weight (M_w) and number average molecular weight (M_n) were determined by gel permeation chromatography (GPC). The samples were prepared by dissolving 30 mg of polymer in 10 ml of THF. The measurements were performed at $T = 25°C$ using a Waters apparatus including a Waters 515 pump, a Waters 717 plus autosampler, a differential refractometer Waters 410, and Styragel columns HR3 and HR 3E (5 µm particles). Each experiment elapsed nearly 1 hour with a flow rate of 1 mL/min. This analysis led to the determination of the molecular weights using a calibration performed with PS standards. Polydispersity values were calculated as 1.05 for PS and 1.024 for dPS.

2.2. *Sample Preparation*

Sample preparation of polymer/LC materials was made following a combination of solvent induced phase separation and thermal induced phase separation techniques [10]. The polymer and the LC were dissolved in THF which is a common organic solvent at a weight fraction of 50% for the polymer at room temperature. The resulting mixtures were stirred mechanically for 2 h. A small quantity of the mixture was cast on a clean glass slide before drying for 24 h. After complete evaporation of THF, another glass slide was put on top of the first one.

2.3. *Polarizing Optical Microscopy*

The thermo-optical studies were performed on a POM Jenapol, equipped with a heating/cooling stage Linkam THMS 600 and a Linkam TMS 92 temperature control unit. The samples underwent a heating ramp of 1°C/min from room temperature to 15 degrees above the transition temperature to the isotropic state (ramp 1 up). They were left for 5 min in the isotropic state before cooling down below room temperature at a rate of $-1°C$/min (ramp 1 down). Five minutes later, a second heating ramp was applied at a rate of 1°C/min (ramp 2 up). The sample was kept for 5 min in the isotropic state and cooled down at $-1°C$/min (ramp 2 down). The same heating/cooling cycle was repeated a third time (ramp 3 up and down). Several duplicate samples were prepared following the same procedure in order to check the validity of the results.

2.4. *Differential Scanning Calorimetry*

DSC measurements were performed on a Perkin Elmer Pyris Diamond calorimeter equipped with an Intracooler 2P system allowing cooling experiments. Samples for calorimetric measurements were prepared by introducing approximately 8 mg of the sample into aluminum DSC pans, which have been sealed to avoid evaporation effects during the temperature treatment. A rate of $10°C/min$ (heating and cooling) was used in the temperature range -70 to $+100°C$. The program consists first in cooling the sample followed by three heating and cooling cycles to take into account eventual thermal events related to the sample preparation history. In each case, at least three duplicate samples having the same composition and prepared independently were used to check the reproducibility of results.

3. Results and Discussion

The phase diagram was constructed by identifying the structures depending on composition and temperature of the binary systems. The observations by POM were carried out while varying the concentration of 8CB, covering the range from 45 to 100% in 8CB. Figure 1 shows the optical micrographs observed under crossed and uncrossed polarizers for pure 8CB and pure dPS. In Figure 1a, the texture of the LC is of the conic focal type, characteristic of the smectic A phase. For the pure dPS matrix the corresponding phase appeared isotropic such as represented in Figure 1b. With exception of a change of light contrast, one does not notice any change from observations conducted with crossed or uncrossed polarizers .

At $25°C$, when 45% of LC was added to the polymer matrix, the micrographs taken under crossed polarizers showed a colored illumination of the objects. One distinguishes several structures from the composite material as it is shown in Figure 2a;

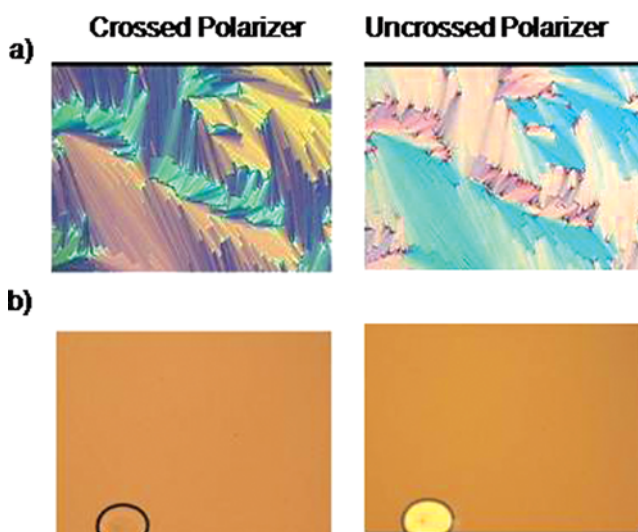**Figure 1.** Optical micrographs observed at $T = 25°C$ under crossed and uncrossed polarizers for a) pure 8CB and b) pure dPS. The ellipsoidal object in the latter case corresponds to an air bubble used as reference. (Figure appears in color online.)

Table 1. Fitting parameters for the two systems dPS 59000/8CB and PS 44000/8CB

Systems	N_1	N_2	A	B
dPS 59000/8CB	1	38	−2.93	1179.98
PS 44000/8CB	1	32	−2.408	1010.76

especially the LC confined in domains, which appears as focal conic texture of the smectic A phase. The uncolored part corresponds to the polymer.

When rising the temperature, the isotropic-isotropic phase appeared as shown in Figure 2b. In this case, the LC lost its birefringence and thus became transparent. Nevertheless, at $T = 41°C$, there was a segregation of the mesogen from the polymer which is illustrated by the colorless circular domains.

From all these considerations, the phase diagram of dPS 59000/8CB was constructed while analyzing each composition for the mixtures undergoing a constant reduction of the temperature, i.e., related to the slope of the first cooling ramp. The corresponding morphological analysis is displayed in the Figure 3. The construction of the phase diagram was completed by DSC measurements; in this case the analysis was carried out on the first heating ramp. The phase diagram shows a dissymmetrical form of "upper critical solution temperature" (UCST) type with four distinct areas. Beyond a certain critical temperature called T_c, the mixture forms only one homogeneous phase consisting of a single isotropic phase (I). The other parts of the diagram exhibit three domains depending essentially on the temperature: isotropic + isotropic (I + I), nematic + isotropic (N + I) and smectic A + isotropic (S + I). The nematic and smectic phases in Figure 3 vary slightly with composition and the obtained values for T_{NI} (nematic-isotropic transition temperature of the LC) and T_{SN} (smectic A – nematic transition temperature of the LC) were very close to those obtained from pure 8CB; but they seem to overlap when approaching the concentration of 45% of 8CB. With this concentration, the nematic phase was hardly visible; and the limit of resolution of the POM technique did not allow distinguishing the smectic A phase from the nematic one. This behavior was different for the PS 44000/8CB system where around a concentration of 35% of 8CB, only the smectic A phase was observed. It should be noted that this latter system was the subject of a former study where the effect of molecular weight was examined in an
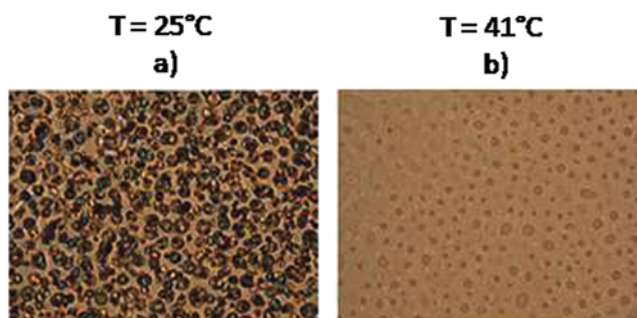

Figure 2. Morphological changes observed during heating of the 45% 8CB/55% dPS mixture showing: a) isotropic + smectic A coexistence regions at $T = 25°C$ and b) isotropic + isotropic coexistence regions at $T = 41°C$. (Figure appears in color online.)
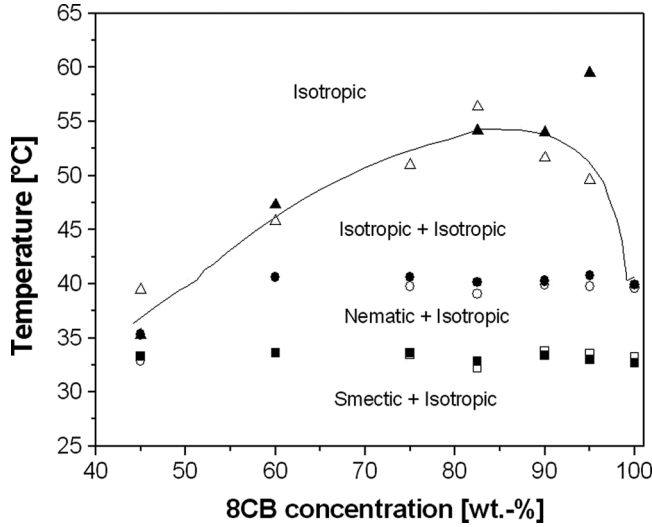
Figure 3. Equilibrium phase diagram of dPS59000/8CB. The solid symbols in this diagram represent experimental data obtained by POM (corresponding to the first cooling ramp) while the empty symbols represent experimental data obtained by DSC (corresponding to the first heating ramp). The solid line is a guide for the eyes.

exhaustive way [11]. The effect of polymer length on the thermodynamic behavior of acrylate/octylcyanobiphenyl mixtures was considered as well [12].

A more detailed analysis of the experimental data can be performed with the help of a theoretical framework describing the phase behavior. The theoretical formalism used to describe the phase behavior of a mixture of linear polymer and LC with smectic A – nematic and nematic - isotropic transitions was reported in the literature [13,14].

The calculations were made starting from a free energy model f representing the sum of the Flory-Huggins free energy of isotropic mixing $f^{(i)}$ and the Maier-Saupe-McMillan free energy of anisotropic ordering $f^{(n)}$. These free energies are recalled without further details for shortness.

$$\frac{f^{(i)}}{n_0 k_B T} = \frac{\varphi_1 \ln \varphi_1}{N_1} + \frac{\varphi_2 \ln \varphi_2}{N_2} + \chi \varphi_1 \varphi_2 \tag{1}$$

and

$$\frac{f^{(n)}}{n_0 k_B T} = \frac{\varphi_1}{N_1} \left[-\ln Z + \frac{1}{2}\nu \varphi_1 (S^2 + \xi \sigma^2) \right] \tag{2}$$

The subscripts 1 and 2 refer to smectic A LC and polymer network, respectively. Thus φ_1 and φ_2 are their respective volume fractions. The Flory-Huggins isotropic mixing interaction parameter was taken to be an inverse function of temperature of the form:

$$\chi = A + \frac{B}{T} \tag{3}$$

where A and B are constants independent of T. They are chosen to obtain the best fit with the experimental data in the part of the diagram where the isotropic interaction is most significant. In Eq. (2), S and σ are, respectively, nematic and smectic A order parameters which are very important to know to establish the phase diagram.

$$S = \frac{1}{2}\left[3\langle\cos^2\theta\rangle - 1\right] \qquad (4)$$

$\langle\ldots\rangle$ in Eq. (4) denotes the average with respect to the orientation distribution function. θ is the angle between a reference axis, which corresponds to the long molecular axis, and the director of the LC [16,17].

$$\sigma = \frac{1}{2}\left\langle(3\cos^2\theta - 1)\cos\frac{2\pi z}{d}\right\rangle \qquad (5)$$

$\langle\ldots\rangle$ in Eq. (5) represents the average with respect to the distribution of angle θ and coordinate z (along the direction of the smectic order), and d is the distance between consecutive smectic layers. The normalized partition function Z is related to the nematic and smectic orders:

$$Z = \iint d\mu\,dz\,\exp\left[\frac{m_n}{2}(3\mu^2 - 1)]\right]\,\exp\left[\frac{m_s}{2}(3\mu^2 - 1)\cos 2\pi\frac{z}{d}\right] \qquad (6)$$

where m_n and m_s are the mean field parameters rising from the minimization of the anisotropic energy in terms of the order parameters S and σ.

$$m_n = \nu S\varphi_1 \quad m_s = \xi\nu\sigma\varphi_1 \qquad (7)$$

where ν is the Maier-Saupe quadrupole interaction parameter and ξ is the strength of smectic interaction in the McMillan model.

$$\nu = 4.54\frac{T_{NI}}{T} \qquad (8)$$

ξ depends on the ratio T_{SN}/T_{NI}. In order to model the part of the experimental points of the phase diagrams of dPS/8CB system, one should determine N_1, N_2, A, B, ν, and ξ.

As the maximum of the binodal corresponds to a critical temperature T_c and a critical volume fraction φ_c, we can deduce N_2, which is the number of repetition units of polymer from Eq. (9) by considering $N_1 = 1$ since the LC is a single molecule.

$$\varphi_{1c} = \frac{\sqrt{N_2}}{\sqrt{N_1} + \sqrt{N_2}} \qquad (9)$$

Constants A and B of the interaction parameter are connected to the critical temperature according to Eqs. (10) and (11).

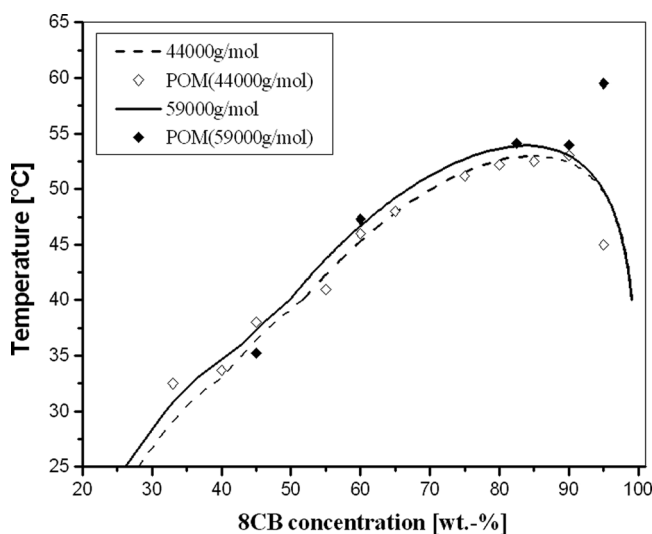$$\chi_c = \frac{1}{2}\left(\frac{1}{\sqrt{N_1}} + \frac{1}{\sqrt{N_2}}\right)^2 \qquad (10)$$

Figure 4. Phase diagrams of two systems dPS 59000/8CB and PS 44000/8CB. Solid and empty symbols correspond to POM measurements for dPS/8CB and PS/8CB systems, respectively. The solid and dashed curves represent the theoretical predictions obtained using the fitting parameters from Table 1.

$$B = \frac{\chi_c - A}{T_c} \tag{11}$$

If the critical temperature is known experimentally, B can be expressed in terms of A implying that just only one adjustable constant A is needed to fit the data. In the phase diagram of the UCST type, the highest absolute negative value of A, corresponds to the broadest gap of miscibility $(I + I)$ [15]. A was adjusted in order to obtain a good agreement between the experimental and theoretical results.

Various parameters obtained for the dPS/8CB system are gathered in the table together with those obtained in the literature for a PS/8CB system [13]. ν and ξ were determined from calorimetric studies which allow to get precise nematic-isotropic and smectic A-nematic transition temperatures.

To illustrate the C–D bond effect on the phase behavior of the two systems, Figure 4 shows both phase diagrams plotted with the same scale. The solid and the empty symbols correspond to the POM measurements for dPS/8CB and PS/8CB systems, respectively. Solid and dashed curves represent calculated binodals.

The critical point agrees well to the theoretical prediction. A larger miscibility gap appeared with dPS probably since it has a slightly higher molecular weight than PS. Clear isotropic to nematic to smectic A to crystalline sequences were found. These sequences took place at the same temperatures, not taking into account neither the chemical structure of the PS nor its size, supporting the view that the ordered phases were made of pure LC.

4. Conclusions

The construction of experimental phase diagrams dPS 59000/8CB and PS 44000/8CB was carried out by optical microscopy (POM), supplemented by data from

calorimetry. The morphology of the domains has been established and shows a strong dependence on the composition of the system. The phase diagrams exhibit one homogeneous isotropic phase (I) and three biphasic phases $(I + I)$, $(N + I)$ and $(S + I)$. They were analyzed with a theoretical model combining the Flory-Huggins theory of isotropic mixing and the Maier-Saupe-McMillan theories of anisotropic order. The choice of deuterated polystyrene for a fundamental analysis not only makes it possible to increase contrast during neutron scattering experiments, but it also facilitates the distinction between the absorption bands of C–D and C–H bonds by infrared spectroscopy. This part of work is currently under investigation.

References

[1] Simoni, F. *et al.* (1995). *Non-linear Optical Properties of Liquid Crystals and Polymer Dispersed Liquid Crystals*, World Scientific: Singapore.

[2] Crawford, G. P., Zumer, S. (1996). *Liquid Crystal in Complex Geometries*, Taylor and Francis: London.

[3] Mucha, M. (2003). *Prog. Polym. Sci.*, *28*, 837.

[4] Higgins, D. A. (2000). *Adv. Mater.*, *12*, 251.

[5] Formentin, P., Palacios, R., Ferré-Borrull, J., Pallares, J., & Marsal, L. F. (2008). *Synthetic Metals*, *158*, 1004.

[6] Flory, P. J. (1965). *Principles of Polymer Chemistry*, Cornell University Press: Ithaca, NY.

[7] Maier, W., & Saupe, A. (1959). *Z. Naturforschung*, *14a*, 882.

[8] Maier, W., & Saupe, A. (1960). *Z. Naturforschung*, *15a*, 287.

[9] McMillan, W. L. (1971). *Phys. Rev. A*, *4*, 1238.

[10] Doane, J. W. (1990). Polymer dispersed liquid crystals, 361–395. In *Liquid Crystals: Their Applications and Uses*, Bahadur, B. (Ed.), World Scientific, Singapore, Vol. 1.

[11] Benmouna, F., Daoudi, A., Roussel, F., Leclercq, L. J., Buisine, M., Coqueret, X., Benmouna, M., Ewen, B., & Maschke, U. (2000). *Macromolecules*, *33*, 960.

[12] Crawford, N., & Dadmun, M. D. (2006). *Liquid Crystals*, *33*(2), 195.

[13] Benmouna, F., Coqueret, X., Maschke, U., & Benmouna, M. (1998). *Macromolecules*, *31*, 4879.

[14] Benmouna, R., & Benmouna, M. (2010). *J. Chem. Eng. Data*, *55*, 1759.

[15] Kyu, T., Shen, C., & Chiu, H.-W. (1996). *Mol. Cryst. Liq. Cryst.*, *287*, 27.

[16] Khoo, I. C. (2007). *Liquid crystals*, 2nd edition, Wiley&Sons.

[17] Pedrotti, F. L., Leno, S. J., & Pedrotti, S. (2008). *Introduction to optics*, 2nd edition, chapter 14, Prentice Hall.